Transactions of the **14th International Conference on Structural Mechanics in Reactor Technology** (SMiRT 14), Lyon, France, August 17-22, 1997 **G13/2**

# Creep fatigue crack growth on CT25 specimens in an 316L(N) stainless steel at 650°C

**Polvora J.P.(1), Drubay B.(1), Piques R.(2), Laiarinandrasana L.(2), Martelet B.(3)**
*(1) CEA, France*
*(2) Ecole des Mines de Paris, France*
*(3) EDF, France*

## ABSTRACT

Creep fatigue crack growth tests in an 316L(N) stainless steel were carried out on CT specimens at 650°C with tensile holdtimes ranging from ½ h to 24h. Experimental crack growth rates, da/dN, are modelled using a linear summation of cyclic and creep contributions. A good agreement is obtained using a fracture mechanics creep parameter $C^*_s(t)$, estimated from a reference stress approach, which continuously takes into account the effects of primary and secondary creep during the tests.

## 1. INTRODUCTION

The integrity of components operating at elevated temperatures is an important concern for the nuclear industry. Failure in engineering structures is generally caused by several complex mechanisms including creep, fatigue and also aggressive environments. To ensure the reliability of these components, a quantitative evaluation of the crack growth behavior under creep and creep-fatigue conditions is needed. In recent years, there have been a number of investigations concerning initiation and growth of cracks subjected to creep-fatigue loadings in austenitic stainless steels, such as 304 or 316. These studies have led to a widespread use of the fracture mechanics parameter C*, initially proposed by Landes and Begley [1]. More recently, Jaske [2] has shown that it is a reliable parameter to characterize creep crack growth in 316L steels and generally in ductile materials.
Initially restricted to stationary cracks and extensive creep conditions, the use of C*-integral has been generalized, with certain limitations, to the case of slow moving cracks and transient creep conditions including small scale creep, primary creep and secondary creep. Different simplified methods for the estimation of C* have been developed in defect assessment rules including the A16 guide [3] or the R5 procedure [4]. In creep-fatigue conditions these methods are generally based on simple summation rules calculating the respective contributions of fatigue and creep propagation to the total crack growth. Although these methods can give reasonably reliable estimates of the crack growth, an over-conservatism is often obtained. Furthermore, they fail to predict some peculiar growth rate behaviors due to primary creep effects such as initial crack decelerations.

In this paper, creep and creep-fatigue tests results, performed at CEA Saclay within an important program named PROFIS are presented. Creep fatigue crack growth (CFCG) data were obtained at 650°C using CT specimens subjected to trapezoidal loading waveforms with holdtimes ($T_h$) ranging from ½ h to 24h. A new method of crack growth prediction for creep fatigue conditions is proposed based on an improvement of the A16 guide procedure. The estimation of the macroscopic parameter $\dot{C}^*s(t)$ and its integration during the test is conducted in order to take into account the continuous effects of creep during the full test duration.

## 2. MATERIAL AND EXPERIMENTAL PROCEDURE

The material used in this study is an austenitic stainless steel (316L(N)) provided as a 30mm thick rolled plate, annealed at 1100°C and water quenched. The chemical composition of this steel is presented in table 1. It has been already studied in a previous program named AMORFIS[5].

Table 1 : Chemical composition of 316 L (N) (%weight)

| C | Cr | Ni | Si | Mo | Ta | Mn | N | Cu | Ti | Nb | Co | S | P |
|---|---|---|---|---|---|---|---|---|---|---|---|---|---|
| 0.02 | 17.51 | 12.2 | 0.35 | 2.35 | 0.01 | 1.76 | 0.071 | 0.13 | 0.004 | 0.005 | 0.11 | 0.004 | 0.002 |

All crack growth tests were performed using standard compact tension specimens (CT) with a width W=50, a crack length ratio a/W≥0.55 and a thickness B=25mm. The creep specimens are 20% side-grooved with a net thickness $B_{net}$ =20mm. All specimens were fatigue pre-cracked at room temperature with final ΔK values always lower than the initial ones at high temperature tests. Load point displacements, δ, were measured using an extensometer attached to the specimen. Crack lengths, a, as a function of time were determined using a DC-potential drop method and a calibration curve between Δa and DC-potential. Creep and creep-fatigue tests with their respective loading conditions are listed in table 2 and table 3.

Table 2 : Creep test conditions at 650°C

| Specimen | F (kN) | a/W | T(°C) | Δa (mm) | $T_i$ (h) | Test duration(h) |
|---|---|---|---|---|---|---|
| 86 | 14.25 | 0.59 | 650 | 7.65 | 20 | 1100 |
| 87 | 13.25 | 0.57 | 650 | 1.1 | 90 | 3950 |

Table 3 : Creep-Fatigue test conditions at 650°C

| Specimen | ΔF (kN) | a/W | T (°C) | $T_h$ (h) | Δa (mm) | Test duration (h) |
|---|---|---|---|---|---|---|
| 80 | 13 | 0.57 | 650 | 0.5 | 0.99 | 302 |
| 81 | 9 | 0.55 | 650 | 0.5 | 0.55 | 470 |
| 82 | 11 | 0.56 | 650 | 5 | 0.58 | 1215 |
| 83 | 10 | 0.57 | 650 | 5 | 0.208 | 370 |
| 91 | 11 | 0.57 | 650 | 5 | 2.57 | 5700 |
| 90 | 13 | 0.57 | 650 | 12 | 3.6 | 3400 |
| 93 | 14 | 0.59 | 650 | 24 | 5.88 | 1350 |

All tests were carried out at 650°C under load controlled conditions using two servo-mechanical testing machines (Walter&Bai and Mayes) with imposed creep and trapezoidal creep-fatigue loading. The loading-unloading duration is 14s and the dwell times vary from ½h to 24 h. All creep fatigue tests were performed at the loading ratio of R=0.1.

## 3.RESULTS

### *3.1 Creep Crack growth*

Figure 1 shows the load line displacement, δ, and the increment of crack length, Δa, as a function of time for the specimen CT87 tested in pure creep. This superposition plot reveals the similitude of both behaviors. The crack length is directly influenced by the creep deformation laws. After an initial high value, the crack growth rate starts to decrease during a transient which can last almost 25% of the life time specimen. This phenomenon, also reported by Riedel [6] for 2 ¼ Cr-1Mo steels, is attributed to primary creep effects, particularly important for this type of 316L(N) steel. During this transitional phase, crack initiation generally occurs. The time to initiation, $T_i$, reported in table 2 is defined as the time necessary for the crack to grow over a distance of 50μm. It can be noticed that this time is very short in comparison with the life time of the specimen.

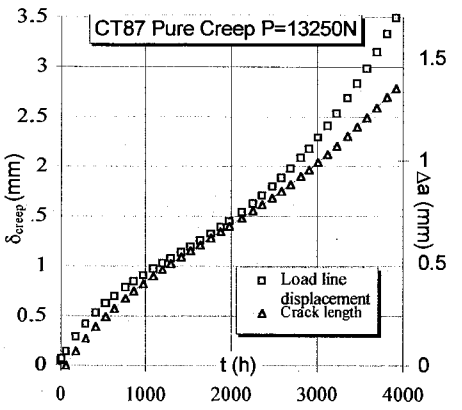


Figure 1 : Evolution of crack length and load line displacement in a pure creep test

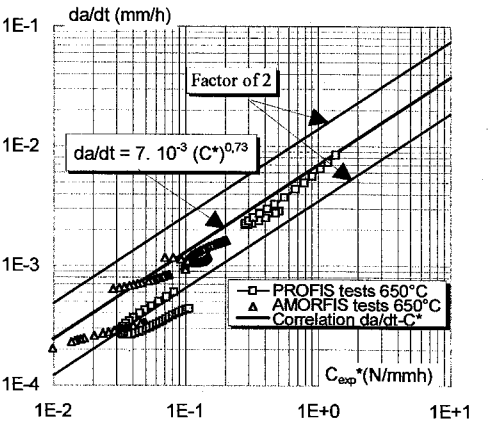


Figure 2 : Creep crack growth at 650°C correlated using C*

Crack growth rates da/dt are reported in figure 2 as a function of the parameter $C^*_{exp}$, evaluated during the tests according to the ASTM 1457-94 recommendations :

$$C^*_{exp}(t) = \eta \frac{n_2}{n_2 + 1} \frac{P\dot{\delta}}{B_{net}(W-a)} \qquad (1)$$

Where $\dot{\delta}$ is the creep displacement rate, $n_2$ the secondary creep law exponent ($\dot{\varepsilon} = B_2\sigma^{n_2}$), P the applied load and $\eta$=2 + 0.52(W-a)/W for CT specimens. Two creep tests from the PROFIS program as well as four tests from the AMORFIS program [5] are also reported in figure 2. A correlation, with a slight reasonable scatter band, is obtained between da/dt(mm/h) and C*(N/mmh) :

$$\frac{da}{dt} = 7.10^{-3}\left(C^*_{exp}\right)^{0,73} \qquad (2)$$

This relation is in good agreement with previous studies concerning 316L steel for temperatures ranging from 550°C to 650°C [1,7]. It can be noticed that a similar trend is obtained during the transition phase even if $\dot{a}$ and C* are decreasing.

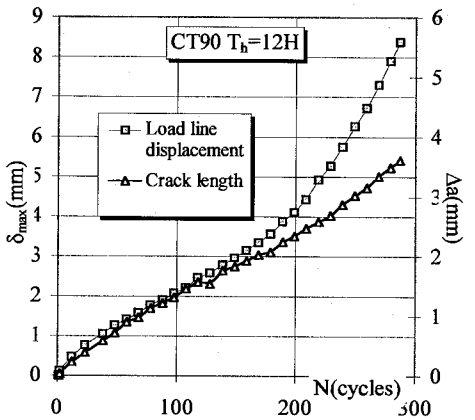


Figure 3 : Evolution of crack length and load line displacement in a creep-fatigue test

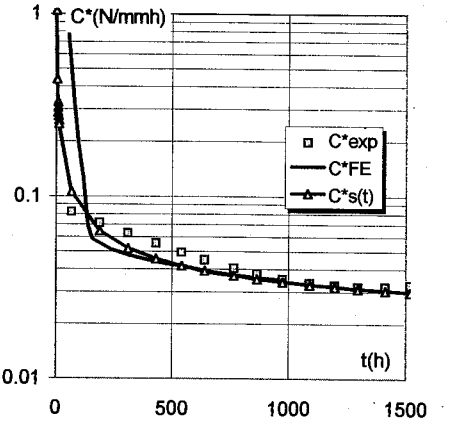


Figure 5 : Comparison between experimental, analytical and numerical estimations of C*

*3.2 Creep fatigue crack growth*

The trend observed in pure creep is also obtained in creep-fatigue when comparing the evolution of δ and Δa as a function of the number of cycles N (figure 3). For dwell times greater than 0.5h, the crack length follows the load line displacement curvature indicating that the cracking process is principally time dependent. SEM observations of fracture surfaces have revealed intergranular crack propagation for holdtimes more than 0.5 hour. For holdtimes less than 0.5h, this is to be verified. In figure 4, the crack growth rate da/dN is plotted as a function of the stress intensity factor range ΔK. The experimental data is compared with the material Paris law derived from continuous fatigue tests performed on standard compact tension specimens at 650°C (da/dN=C $\Delta K^m$, where C=3.2 $10^{-7}$ and m=2.46). The results support the view that, for the same value of applied ΔK, crack growth rate increases with increasing hold times. Two situations however have to be distinguished :

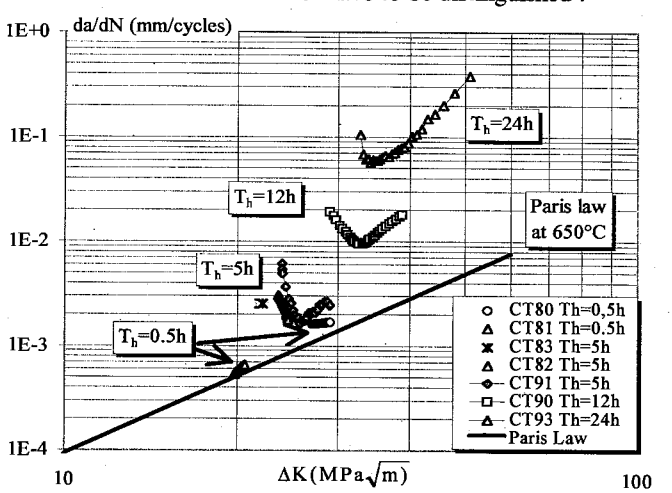


Figure 4 : Crack growth rate, da/dN, as a function of ΔK, for different hold times

Firstly, for the short holdtimes ($T_h$=0.5h), crack growth rates slightly increase in comparison with pure fatigue data (about 50%). The curve remains almost parallel to the Paris Law. Secondly, for $T_h \geq$5h, the crack growth rate behaviors are similar to those obtained in pure creep. After an initial high value, da/dN starts to decrease, reaches a minimum and increases again with a slope higher than the Paris law. This singular behavior (not often analyzed or interpreted in the literature) correlates well with data reported in a recent European compilation of tests on 316L(N) austenitic stainless steel [8]. It concerns some creep-fatigue tests with holdtimes ranging from 1h to 10h.

## 4. DISCUSSION

### *4.1 Estimation of crack tip parameters governing crack growth*

An estimation of C*-integral can also be obtained using the reference stress method initially introduced by Ainsworth [9] for the estimation of J. An extension of this method to creep conditions leads to the definition of the parameter $C^*_S(t)$ defined, for example in the A16 guide [3], as:

$$C^*_S(t) = J_e \frac{\dot{\varepsilon}_{ref} E}{\sigma_{ref}} \quad (3)$$

where $J_e = (K^2/E^*)$ is the elastic value of J and $E^*=E$ or $E^*=E/(1-\nu^2)$, respectively in plane stress and in plane strain conditions. $\dot{\varepsilon}_{ref}$ is the creep strain rate at the reference stress $\sigma_{ref}$, obtained from uniaxial creep curves. $\sigma_{ref} = P/(BWm(a/W))$, where m(a/W) is obtained from limit load analysis [10] for Von Mises and plane strain conditions. Eqn. (3) is not restricted to secondary creep behavior. It can be applied in conditions varying from primary creep to tertiary creep. Therefore, it can be used to estimate C* in any component for which stress intensity factor K solutions are available.
Experimental values of C* from CT87 pure creep test are compared in figure 5 with $C^*_S(t)$ estimate and with Finite element calculations of the C*-integral using the CASTEM 2000 finite element code developed at CEA. For the side grooved specimens, $B_{eff}=\sqrt{BB_{net}}$ has been chosen instead of $B_{net}$ for $\sigma_{ref}$ estimations and finite element calculations. This effective thickness is the only one able to describe the global loading as well as the deformation creep behavior of the specimen (assuming plane strain conditions). Figure 5 shows that both estimations are in good agreement with C*-integral contour calculations.

### *4.2 Modelling creep-fatigue crack growth rate*

Creep fatigue growth rate is obtained from a simple summation of the fatigue contribution (cycle dependent) and the creep contribution to the total crack growth :

$$\frac{da}{dN} = \left(\frac{da}{dN}\right)_{fat} + \left(\frac{da}{dN}\right)_{creep} \quad (4)$$

No specific interaction between the damage mechanisms of creep and fatigue is included in the proposed model. Moreover, the actualization of the crack length at each cycle was taken into account. The fatigue contribution, for one cycle, is obtained using the Paris law deduced from continuous fatigue tests :

$$(\Delta a)_{fat} = C(\Delta K)^m \quad (5)$$

The creep contribution, for one cycle, is obtained by continuous integration (between t and $t+T_h$) of the $\dot{a} = f(C^*)$ correlation (Eqn. (2)) deduced from pure creep tests :

$$(\Delta a(t))_c = \int_t^{t+T_h} A \cdot \left(C_s^*(t)\right)^q \cdot dt \quad \text{or} \quad (\Delta a(N))_c = \int_N^{N+1} A \cdot \left(C_s^*(NT_h)\right)^q \cdot T_h dN \quad (6)$$

In this relation, $C^*_S(t)$ depends only on $\dot{\varepsilon}_{ref}$ which is the creep strain rate at the reference stress $\sigma_{ref}$. $\varepsilon_{ref}$ is obtained by a linear decomposition of strain using the primary and secondary creep law parameters as proposed in the RCC-MR code [11] :

$$\begin{cases} \varepsilon_{ref} = B_1 \sigma_{ref}^{n_1} t^{p_1} & t < T_{TR} \\ \varepsilon_{ref} = B_1 \sigma_{ref}^{n_1} T_{TR}^{p_1} + B_2 \sigma_{ref}^{n_2} (t - T_{TR}) & t \geq T_{TR} \end{cases} \quad (7)$$

Where $T_{Tr}$ is the transition time between primary and secondary creep, defined as the time when the primary strain rate equals the secondary strain rate:

$$t_{TR} = \left[ \left( B_2 \sigma_{ref}^{n_2 - n_1} \right) / (p_1 B_1) \right]^{1/(p_1 - 1)} \quad (8)$$

In Eqn.(7), $\dot{\varepsilon}_{ref}$ is not re-initialized at the beginning of each hold period assuming that the accumulated creep strain is not removed by cyclic plasticity. Therefore, creep damage history is taken into account. This assumption is consistent with the observations made in figures 1 and figure 3 where the load line, δ, and crack length, Δa, are significantly influenced by the creep deformation behavior. This type of modelization has been successfully investigated by Adefris and Saxena [12] using $C_t$ parameter for a 1Cr-1Mo-1/4 V steel.

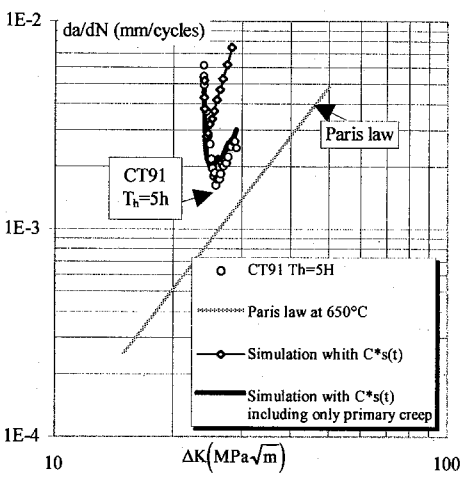


Figure 6 : Comparison between experimental and predicted crack growth rate using Eqn. (4)

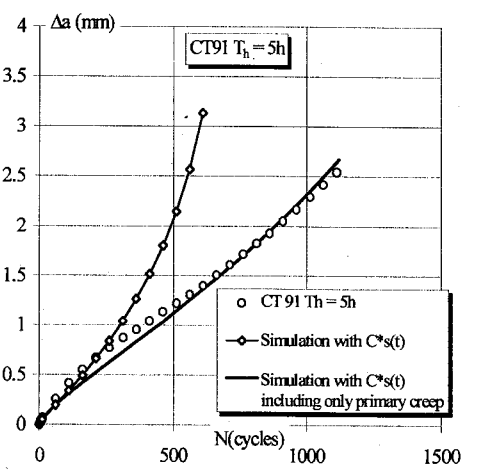


Figure 7 : Comparison between experimental and predicted crack growth using Eqn. (4)

A simulation of creep-fatigue crack growth of specimen CT91 ($T_h$=5h) is presented in figures 6 and 7. This simulation is able to predict the transitional phase of deceleration but the transition between primary and secondary creep appears to be underestimated by $T_{TR}$ ($T_{TR}$=200h) in comparison with the experimental time estimated to 1500h. Smith [13] has

shown that when a 316 type steel is strain hardened at high temperature, the resulting creep behavior is different from the as-received steel. Secondary creep transition appears to be shifted for longer times and for a limit case does not take place. A simulation including only primary creep, in C*s(t) calculation, gives good crack growth predictions. An experimental parameter, $C^*_{exp}(\delta_{Th})$, using the load line displacement increment measured during the dwell, can also be used in simulation( figure 8) instead of C*s(t) for CT93 ($T_h$=24h) specimen:

$$C^*_{exp}\left(\delta_{T_h}\right) = \eta \frac{n_2}{n_2+1} \frac{P\delta_{T_h}}{B(W-a)T_h} \tag{8}$$

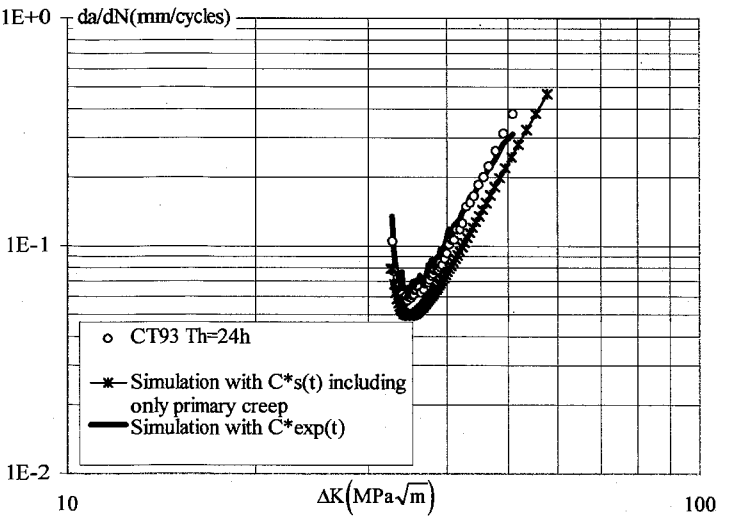


Figure 8 : Comparison between experimental and predicted crack growth rate using Eqn (4) with an analytical or experimental estimation of C*.

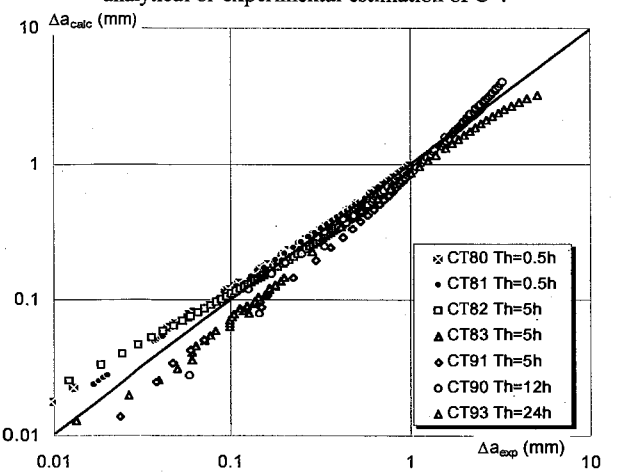


Figure 9 : Comparison between experimental and predicted crack growth using Eqn (4) and Cs*(t) including only primary creep.

A comparison between estimated and experimental crack length is presented in figure 9, for all creep-fatigue tests, with $C^*_s(t)$ including only primary creep strain rates. A fairly good

correlation is obtained even if a slight non-conservatism appears for the longest holdtime. The transition time to secondary creep should be taken into account for very long times, but it cannot be estimated using uniaxial creep laws from « as received material ». Further work is required to take into account the effect of hardening under cyclic creep laws.

## 5. CONCLUSIONS

1. Two pure creep and seven creep fatigue crack growth tests (with tensile hold periods ranging from 0.5h to 24h) in an 316L(N) stainless steel were carried out on normalised CT25 specimens at 650°C under load control conditions.
2. Comparisons between crack growth and load line displacement have shown that the cracking process in creep and creep-fatigue conditions is significantly influenced by the material deformation creep laws.
3. Creep-fatigue crack growth rates, da/dN, are higher than pure fatigue growth rates and increase with increasing holdtime. For long test dwells ($t_h > 5h$), da/dN starts to decrease to a minimum value and increases with a slope higher than the one corresponding to the Paris law. Experimental growth rate is modelled using a phenomenological approach based on a linear summation of cyclic and creep contributions. A good agreement is obtained using a fracture mechanics creep parameter $C^*_S(t)$, estimated with a reference stress approach, which continuously takes into account the effects of primary and secondary creep during the full period of the tests.
4. The experimental transition time between primary and secondary creep is under-estimated by using the material creep laws due to cyclic hardening effects. Further investigations are needed in order to take it into account in the proposed crack growth model.

## REFERENCES


1. Landes, J. D. And Begley, J. A. 1979. ASTM STP 590, Philadelphia, pp.128-148.
2. Jaske, C. E. 1988. ASTM STP 945, Philadelphia, pp. 867-877.
3. Drubay, B and al. 1993. «Defect assessment procedure: A French approach for fast breeder reactors», PVP-Vol. 266. Creep, Fatigue evaluation and Leak-Before-Break Assessment.
4. Assessment Procedure R5, Issue 1. 1990.« An Assessment Procedure for the High Temperature Response of Structures », Nuclear Electric plc.
5. Laiarinandrasana, L. 1996. « High temperature crack initiation in an austenitic stainless steel », Rapport CEA-R-5692 (E), CEA Saclay.
6. H. Riedel. 1987. « Fracture et High Temperature », Springer Verlag, Berlin.
7. Piques, R. 1989.: « Mécanique et mécanismes de l'amorçage et de la propagation des fissures en viscoplasticité dans un acier inoxydable austénitique ». Thèse de doctorat de L'Ecole Nationale Supérieure des Mines de Paris en Sciences et Génie des Matériaux.
8. Huthmann, H., Curbishley, I., Piques, R., Smith, D.J., Data compilation. Report KWU NT-4/93/016. Bergisch Gladbach, 1993.
9. Ainsworth, R. A. 1984. Engn. Fract. Mech. Vol. 19. N°4. p.633-642.
10. Miller, A. G. 1988. Int. J.Press. Vess. and Piping.Vol.32, pp197-327
11 RCC-MR: « Règles de conception et de construction des matériels mécaniques des îlots nucléaires RNR ». 1993. Edition AFCEN.
12. Adrefris, N and Saxena, A. 1996. Fatigue. Fract. Engng. Mater. Struct. Vol 19, No.4, pp.401-411.
13. Smith, D. J, Ellison, E. G. Int. 1992. J.Press. Ves. Piping, Vol 50, pp 231-241.